

Mobility of Bodies in Contact—II: How Forces are Generated by Curvature Effects?

Elon Rimon (elon@robby.caltech.edu) Joel Burdick (jwb@robby.caltech.edu)
Dept. of Mechanical Engineering, CALTECH, Mail Code 104-44, Pasadena, CA 91125

Abstract

We investigate the contact forces generated by 2nd order effects for a body B , in frictionless contact with finger bodies A_1, \dots, A_k . A simple paradox shows that rigid body models are inadequate to explain how contact forces are generated by 2nd order effects. A class of configuration-space based elastic deformation models are introduced, and are shown to explain the restraining forces produced by surface curvature. Using these elastic deformation models, we prove that any object which is kinematically immobilized to 1st or 2nd order is also dynamically locally asymptotically stable with respect to perturbations.

1 Introduction

The 2nd order mobility theory discussed in [12]¹ is kinematic in nature. However, potential applications of 2nd order immobility rely on contact forces generated by surface curvature effects. For example, consider *fixture planning*. The goal is to design fixtures that completely restrain a given object. In the c-space framework of [12], the goal is to completely isolate the object's configuration from the remainder of its freespace, where the fixtures determine the c-obstacles. The frictionless equilibrium grasps of Fig. 1 are work holding examples. $m_{q_0}^1 = 1$ for both grasps, and 1st order theories wrongly predict that the objects are not immobilized. It can be verified that $m_{q_0}^2 = 0$ for both grasps, and the objects are completely immobilized using 2nd order effects. How are the forces which immobilize the object using 2nd order effects generated? We study this problem in this paper.

Using an ideal rigid body model, we relate 2nd order effects to the time-derivative of the contact forces. A simple example, that we term the *Mason Paradox* [7], shows that *ideal rigid body models are inadequate to explain the origin of forces due to 2nd order effects*. Additional assumptions must be introduced to explain these forces. Similar observation, in the context of peg insertion, was made by Rajan et. al [10].

In Section 3 we introduce a class of "lumped parameter" elastic deformation models that are non-linear and admit a c-space based representation. We also introduce a lumped parameter energy loss model that ap-

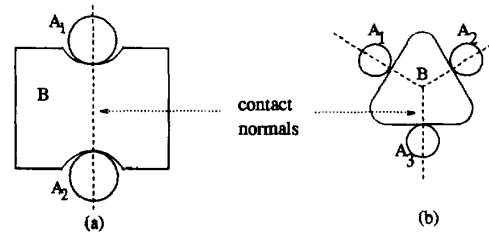


Figure 1. 2nd order immobile grasps

proximately captures the effects of elastic hysteresis during contact deformations. Using these models, we prove that *an object which is (kinematically) immobilized using either 1st or 2nd order effects is (dynamically) locally asymptotically stable*. This stability result justifies the exploitation of 2nd order effects in the practical applications that are discussed in the conclusion.

Other authors have considered elastic deformations or the stability of grasps. For example, Pai and Donald [2] used a linear spring model to study the elastic deformation of snap fasteners. Hanafusa and Asada [5] implemented a stable multi-finger grasp algorithm based on first-order ideas. Montana [8, 9] analyzed the stability of grasps under small perturbation of the contacting fingers.

2 2nd Order Mobility and Rigid Body Models

By an *ideal rigid body model* we mean that no deformation or interpenetration occurs when two bodies are pressed into contact. This section physically interprets 1st and 2nd order free motions, and shows via a paradox that 2nd order effects can not be satisfactorily explained by a rigid body model. In the following propositions, let $A_i(t)$ denote the set of points occupied by finger A_i at time t .

Proposition 2.1 *Let A_i push on B with a non-zero frictionless contact force $F_i(t)$, as B moves along its c-space trajectory $q(t)$. Then $\dot{q}(0)$ is a 1st order escape motion relative to $A_i(0)$ iff the wrench $w(q, F_i)$ satisfies $w(q, F_i) \cdot \dot{q}(0) > 0$. In particular, this implies that the kinetic energy of B increases at $t = 0$:*

$$K(q(t), \dot{q}(t)) > K(q(0), \dot{q}(0)) \quad \text{for all } t \in (0, \epsilon) \quad (1)$$

¹We rely on the terminology and results developed in [12].

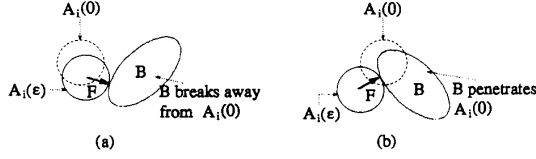


Figure 2. (a) B cannot be stopped along its 1st order escape motions (b) but can be stopped along its 1st order penetration motions

for some $\epsilon > 0$. If $\dot{q}(0)$ is a 1st order roll-slide motion, then $\left. \frac{d}{dt} K(q(t), \dot{q}(t)) \right|_{t=0} = 0$.

Proof: Let \mathcal{CA}_i and its boundary \mathcal{S}_i be associated with $\mathcal{A}_i(t)$ at $t = 0$. It suffices to show that $\left. \frac{d}{dt} K(q(t), \dot{q}(t)) \right|_{t=0} = w(0) \cdot \dot{q}(0) > 0$. According to [12, Theorem 1], $w(0) = \lambda_i(0) \hat{n}_i(q(0))$, where $\lambda_i(0) > 0$ for non-zero finger force. From the definition of the 1st order escape motions it follows that $\dot{q}(0)$ satisfies $\hat{n}_i(q(0)) \cdot \dot{q}(0) > 0$. The last two facts, together with the relation $\dot{K} = w \cdot \dot{q}$, imply the result. \square

In other words, if $\dot{q}(0)$ is a 1st order escape motion relative to $\mathcal{A}_i(0)$, no pushing force realizable by \mathcal{A}_i can decrease B 's kinetic energy during a small time interval $[0, \epsilon]$, nor can \mathcal{A}_i slow B to a halt during this interval (Fig. 2(a)). Conversely, any non-zero force F_i strictly decreases B 's kinetic energy when $\dot{q}(0)$ is a 1st order penetration motion relative to $\mathcal{A}_i(0)$ (Fig. 2(b)).

A physical interpretation of the 2nd order free motions is based on the following proposition:

Proposition 2.2 Let \mathcal{A}_i push on B with a non-zero frictionless contact force $F_i(t)$, as B moves along its c-space trajectory $q(t)$. The pair $(\dot{q}(0), \ddot{q}(0))$ is a 2nd order escape motion relative to $\mathcal{A}_i(0)$ iff $w(q, F_i)$ and its time derivative $\dot{w}(q, F_i)$ satisfy $w(q, F_i) \cdot \dot{q}(0) = 0$ and $\dot{w}(q, F_i) \cdot \dot{q}(0) + w(q, F_i) \cdot \ddot{q}(0) > 0$. This implies that the kinetic energy of B increases at $t = 0$:

$$K(q(t), \dot{q}(t)) > K(q(0), \dot{q}(0)) \quad \text{for all } t \in (0, \epsilon],$$

for some $\epsilon > 0$. If $\dot{q}(0)$ is a 2nd order roll-slide motion, then $\left. \frac{d}{dt} K(q(t), \dot{q}(t)) \right|_{t=0} = 0$ and $\left. \frac{d^2}{dt^2} K(q(t), \dot{q}(t)) \right|_{t=0} = 0$ at $t = 0$.

Proof: From the definition of 2nd order free motions it follows that $\dot{q}(0)$ in the pair $(\dot{q}(0), \ddot{q}(0))$ is a 1st order roll-slide motion. Hence $\dot{q}(0)$ is tangent to \mathcal{S}_i at $q_0 \in \mathcal{S}_i$, and $\left. \frac{d}{dt} K(q(t), \dot{q}(t)) \right|_{t=0} = w(0) \cdot \dot{q}(0) = 0$, by Prop. 2.1. The time derivative of $\dot{K} = w \cdot \dot{q}$ is:

$$\ddot{K} = \dot{w} \cdot \dot{q} + w \cdot \ddot{q}. \quad (2)$$

The wrench due to $F_i(t)$ is given by $w(t) = \lambda_i(t) \hat{n}_i(q(t))$, where $\lambda_i(0) > 0$ for non-zero finger force. Substituting for w and \dot{w} in (2) gives

$$\begin{aligned} \left. \frac{d^2}{dt^2} K(t) \right|_{t=0} &= (\dot{\lambda}_i(0) \hat{n}_i(q_0) + \lambda_i(0) \left. \frac{d}{dt} \hat{n}_i(q(t)) \right|_{t=0}) \cdot \dot{q} \\ &\quad + \lambda_i(0) \hat{n}_i(q_0) \cdot \ddot{q} \\ &= \lambda_i(0) \left\{ \left(\left. \frac{d}{dt} \hat{n}_i(q(t)) \right|_{t=0} \cdot \dot{q} + \hat{n}_i(q_0) \cdot \ddot{q} \right) \right\}, \end{aligned}$$

since \dot{q} is tangent to \mathcal{S}_i at $q_0 = q(0) \in \mathcal{S}_i$. But this is exactly the second-order term in the Taylor expansion of $d_i(q)$ along $q(t)$, given in [12, Eq. 3]. The 2nd order escape motions are defined as the pairs $(\dot{q}(0), \ddot{q}(0))$ that make this term positive. Hence $\dot{K}(0) > 0$. Since $\dot{K}(0) = 0$, it must be that $\dot{K}(t)$ is strictly positive immediately after $t = 0$, which implies the result. \square

Remark: The change in B 's kinetic energy along 2nd order free motions is affected by the pair (w, \dot{w}) , not just w , for we must consider \dot{K} in addition to K . The term $\dot{w} \cdot \dot{q}$ in (2), when \dot{q} is a unit length tangent vector, is exactly the curvature of \mathcal{S}_i along q , at $q_0 \in \mathcal{S}_i$. Thus, \dot{K} along the 2nd order motions depends on the 1st and 2nd order geometry of \mathcal{S}_i at $q_0 \in \mathcal{S}_i$.

The proposition and its proof lead to the following insight. Whenever $\dot{q}(0)$ is a 1st order roll-slide motion and $(\dot{q}(0), \ddot{q}(0))$ is a 2nd order escape motion, \dot{K} is strictly positive during some interval $(0, \epsilon_1]$. Further, according to Prop. 2.1, for a non-zero finger force, $\dot{K}(t) > 0$ if and only if $\dot{q}(t)$ is a 1st order escape motion with respect to $\mathcal{A}_i(t)$. Hence if $(\dot{q}(0), \ddot{q}(0))$ is a 2nd order escape motion, $\dot{q}(t)$ (which is a 1st order roll-slide motion at $t = 0$) must be a 1st order escape motion during $(0, \epsilon_1]$ —i.e., for $t > 0$. However, once $\dot{q}(t)$ becomes a 1st order escape motion, it ceases to be a 1st order roll-slide motion. Thus trajectories of B can be 1st order roll-slide and 2nd order escape motions only at isolated points of time. That is, the only physically realizable motions of B which are continuously 1st order roll-slide motions with respect to $\mathcal{A}_i(t)$ must also be continuously 2nd order roll-slide motions. This insight leads to the following paradox [7].

Mason's paradox: Let B be an ellipse, held by two concave fingers along its major axis (Fig. 3(a)). The fingers push on B with equal and opposite forces, so that the net wrench on B is zero. During $t \in (-\infty, 0)$, the three bodies travel upward with constant velocity. At $t = 0$, the fingers decelerate, in an attempt to bring B to a halt, while maintaining their upward motion, without rotating or sliding sideways. Clearly B must be slowing down with the fingers.

Let us examine the logical conclusion of the rigid body assumption. Let $q(t)$ be B 's c-space trajectory. Since $\dot{q}(t)$ changes only its magnitude, not its direction, and since B is slowing down, it must be true that $\dot{K}(t) < \dot{K}(0)$ immediately after $t = 0$. Since $\dot{q}(0)$ is perpendicular to the fingers' contact forces, it is a 1st order roll-slide motion. According to Prop. 2.1, this implies that $\dot{K}(0) = 0$. Since $\dot{K}(t) < \dot{K}(0)$ immediately after $t = 0$, it must be true that $\ddot{K}(0) < 0$. Indeed, it can be shown that $(\dot{q}(0), \ddot{q}(0))$ is a 2nd order penetration motion with respect to both fingers. According to Prop. 2.2, this implies that $\dot{K}(0) = 0$ and $\ddot{K}(0) < 0$ as expected.

Although 2nd order effects seem to predict the slowing down of B at $t = 0$, a paradox arises at times $t > 0$. $\dot{q}(t)$, being continuously perpendicular to the fingers'

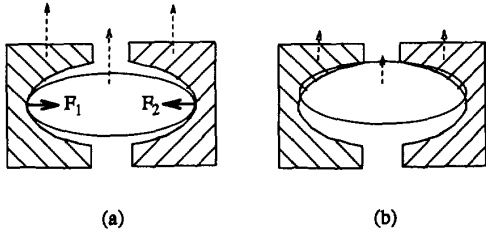


Figure 3. (a) The fingers and object move with uniform velocity. (b) Once the fingers slow down, the object must penetrate the fingers

contact forces, is continuously a 1st order roll-slide motion with respect to the fingers. It follows from Prop. 2.1 that \dot{K} is continuously zero, contradicting the prediction of Prop. 2.2, that $\ddot{K}(0) < 0$ and hence that $\dot{K}(t) < 0$ immediately after $t = 0$.

The contact points must therefore shift their relative position at time $t = 0$. In the rigid body model, this is possible only if the fingers move apart from each other. Otherwise we get interpenetration of the bodies (Fig. 3(b)). We conclude that under the ideal rigid body model, where no interpenetration is allowed, the two fingers cannot slow B down along a purely upward motion. Since practical experience indicates that this conclusion is not true, we must conclude that the rigid body model is inadequate to explain 2nd order effects. In the next section the rigid body idealization is relaxed to allow elastic deformations.

3 Elastic Deformation Contact Models

By an elastic deformation model, we mean a lumped parameter model that relates the deformation of contacting objects to their interbody force. We first establish some properties required for our c-space elastic deformation models.

3.1 The overlap distance

As proposed by Gesley [3], small elastic deformations can be modeled by assuming that the contacting bodies are rigid, but that their volumes are allowed to overlap. This overlap gives rise to a force. To generalize this notion and adapt it to our c-space framework, let $o_i(q)$ be the *overlap* between $B(q)$ and A_i , defined as the minimal amount of translation of B that separates it from A_i (Fig. 4(a)). That is, o_i at configuration $q_0 = (d_0, \theta_0)$ is obtained by minimization of $\|d - d_0\|$ over all translations d such that $B(d, \theta_0)$ and A_i touch each other while their interiors are disjoint.

o_i can be interpreted as a distance function in c-space as follows. Let $S_i|_{\theta_0}$ be the slice of S_i by the c-space hyperplane with fixed orientation θ_0 . Then o_i is:

$$o_i(d, \theta) = \begin{cases} \text{dst}(d, S_i|_{\theta}) & \text{if } q \text{ is inside } CA_i \\ 0 & \text{if } q \text{ is outside } CA_i. \end{cases} \quad (3)$$

Note that o_i is similar to d_i , the Euclidean distance from S_i , except that o_i is positive inside CA_i and is zero

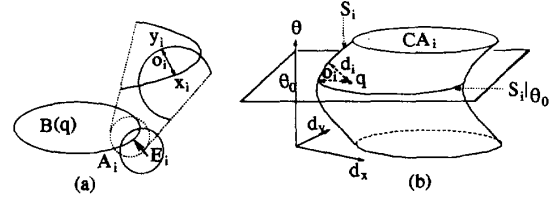


Figure 4. (a) The depth of overlap o_i ; (b) C-space interpretation of o_i

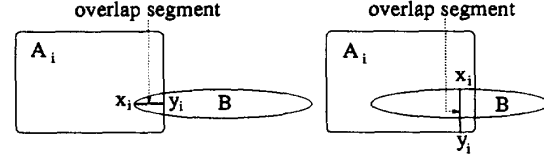


Figure 5. The overlap segment lies in $B \cap A_i$ for small overlaps, but not for deep ones

outside it (Fig. 4(b)). Both o_i and d_i are identically zero on S_i . However, o_i is *non-smooth* on S_i .

o_i is measured with respect to two points, one on the surface of $B(q)$, denoted x_i , and one on the surface of A_i , denoted y_i . x_i and y_i correspond to the points of maximum penetration of the two bodies. Thus, the minimum translation of B that will separate it from A_i occurs along $y_i - x_i$. Thus $o_i = \|y_i - x_i\|$.

Lemma 3.1 *Let x_i and y_i be the points on $B(q_0)$ and A_i where the depth of overlap, $o_i(q_0)$, is achieved. Then $\overline{x_i y_i}$ is perpendicular to the surfaces of B and A_i at its endpoints.*

A proof of this lemma can be found in [11]. For the model to be viable, $\overline{x_i y_i}$ must lie in the intersection of B and A_i .

Lemma 3.2 *For all sufficiently small values of the overlap $o_i(q)$, the overlap segment $\overline{x_i y_i}$ lies wholly inside $B(q) \cap A_i$.*

Fig. 5 shows that the overlap segment may cease to lie in $B(q) \cap A_i$ for “deep” overlaps. However, physically plausible interpenetrations are always small.

We assume that the interbody forces that arise due to elastic deformation can be considered as a single force acting at x_i , pointing into B in the direction $y_i - x_i$. The real-world force acting on B at x_i due to its interpenetration with A_i is denoted $F_i(x_i)$, or F_i for short. Let $\hat{N}(x_i)$ be the inward pointing unit normal to the surface of B at x_i . According to Lemma 3.1, since $\overline{x_i y_i}$ is perpendicular to the tangents of the surfaces of B and A_i , F_i acts in the direction $\hat{N}(x_i)$.

Proposition 3.3 *Let A_i be stationary and let $B(q)$ have overlap $o_i(q) > 0$ with A_i . Let $F(x_i)$ be the inter-body force which arises from an elastic deformation model. If $F(x_i)$ is directed along $\overline{x_i y_i}$ into B , then the corresponding c-space wrench is:*

$$w(q, F_i) = -\|F_i\| \nabla o_i(q),$$

A proof of the proposition is given in [11].

3.2 A Summary of Possible Contact Models

We now summarize different possible elastic deformation contact models.

The Gesley model[3]: In this model, it is postulated that the *magnitude* of F_i depends on o_i and on its rate of change, \dot{o}_i , as follows:

$$\|F_i(x_i)\| = \begin{cases} \eta_i o_i + \xi_i o_i \dot{o}_i & \text{if } o_i > 0 \\ 0 & \text{if } o_i = 0, \end{cases} \quad (4)$$

where $\eta_i, \xi_i > 0$. This is basically a c -space “spring” (with spring constant η) with damping (with damping coefficient ξ). Note, *this is NOT a linear spring model*, since o_i does not in general vary linearly with respect to the displacement of B . The damping term is a simple lumped parameter approximation of energy loss processes that arise from inelastic effects, such as elastic hysteresis. The factor o_i in the damping term ensures that no damping occurs when the bodies do not interpenetrate.

The Hertz Contact model: A more traditional lumped parameter elastic contact model, which has been corroborated in experiments, is due to Hertz (1882) [1]. When interpreted in our c -space framework, it can be shown that the Hertz model produces a contact force of the form (neglecting damping effects):

$$\|F_i(x_i)\| = \begin{cases} \eta_i o_i^{3/2} & \text{if } o_i > 0 \\ 0 & \text{if } o_i = 0, \end{cases} \quad (5)$$

where η_i depends on the elasticity of the bodies and their undeformed contact geometry [1].

A general class of contact models: It can be shown that the c -space wrench corresponding to the Hertz and Gesley models is the negated gradient of the following c -space elastic potential energy function:

$$U_i(q) = \frac{1}{2+p} \eta_i o_i^{2+p}(q) \quad (6)$$

where $p = 0$ in Gesley’s model and $p = 0.5$ in Hertz’s model. More generally, the stability results of Section 4 will hold for any model of the form (6), and in fact for any elastic contact model in which $U_i(q)$ satisfies the two requirements: (1) $U_i(q)$ must be strictly positive for q inside \mathcal{CA}_i , zero on \mathcal{S}_i , and zero outside \mathcal{CA}_i (i.e., the inter-body force increases with increasing deformation); (2) $\nabla U_i(q)$ is Lipschitz continuous.

3.3 A More Realistic Damping Model

The damping-force in Gesley’s model, denoted $D_i(x_i)$ where $D_i(x_i) = \xi_i o_i \dot{o}_i \hat{N}(x_i)$, is crude and is not consistent with tribological studies or physical intuition. For example, it does not account for energy loss in the situation shown in Fig. 6(a). In this example \mathcal{A}_i is stationary, has planar surface, and is soft relative to B . As B translates parallel to \mathcal{A}_i ’s surface, a fixed overlap o_i is maintained. Since $\dot{o}_i = 0$, $D_i(x_i)$ vanishes. However, intuition suggests that inelastic effects due to material displacement caused by the passing of B must result in

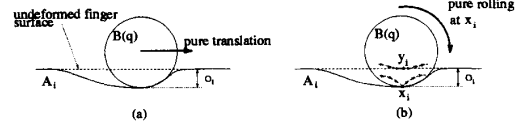


Figure 6. (a) Pure translation with constant o_i (b) Pure rolling with constant o_i

energy loss. We now introduce a comprehensive lumped parameter energy loss model.

Let s_i be the point in B ’s body-frame coordinates that is coincident with y_i :

$$y_i = X(q, s_i) = R(\theta)s_i + d \quad \text{where } q = (d, \theta).$$

Also recall that $x_i = X(q, r_i) = R(\theta)r_i + d$. The velocities $\dot{X}_{r_i} = \dot{R}r_i + \dot{d}$ and $\dot{X}_{s_i} = \dot{R}s_i + \dot{d}$ describe the instantaneous velocity of the body fixed points r_i and s_i in world coordinates. The components of these velocities that are tangential to the surface are given by their projection onto the plane normal to $\bar{x}_i \bar{y}_i$: $[I - \hat{N}_i \hat{N}_i^T] \dot{X}_{r_i}$, and $[I - \hat{N}_i \hat{N}_i^T] \dot{X}_{s_i}$, where \hat{N}_i is short for $\hat{N}(x_i)$. The damping due to $[I - \hat{N}_i \hat{N}_i^T] \dot{X}_{r_i}$ acts at x_i , and the one due to $[I - \hat{N}_i \hat{N}_i^T] \dot{X}_{s_i}$ acts at y_i . The resulting damping forces are:

$$\begin{aligned} D_{i1}(x_i) &\triangleq \xi_i o_i (\dot{o}_i \hat{N}_i - [I - \hat{N}_i \hat{N}_i^T] \dot{X}_{r_i}) \\ D_{i2}(y_i) &\triangleq -\xi_i o_i [I - \hat{N}_i \hat{N}_i^T] \dot{X}_{s_i} \end{aligned} \quad (7)$$

The following lemma (proved in [11]) provides an equivalent expression for D_{i1} and D_{i2} .

Lemma 3.4 *If \mathcal{A}_i is stationary, then $D_{i1}(x_i) = -\xi_i o_i \dot{X}_{r_i}$, and $D_{i2}(y_i) = -\xi_i o_i \dot{X}_{s_i}$.*

A justification for inclusion of the term $D_{i2}(y_i)$ is shown in Fig. 6(b), where B performs pure rolling on a line at a fixed depth o_i . Pure rolling is characterized by $\dot{X}_{r_i} = 0$. Since $\dot{o}_i = 0$ and $\dot{X}_{r_i} = 0$, D_{i1} is identically zero. Yet intuition suggests that material deformation causes damping due to inelastic effects. Indeed, \dot{X}_{s_i} , and consequently $D_{i2}(y_i)$, are non-zero for this motion. Our intuition in this example is backed up by tribological studies [4][pp 177-182], where a term much like $D_{i2}(y_i)$ is derived.

4 Dynamic Stability of Immobilized Objects

We now consider the predictive powers of our kinematic mobility theory when applied to the dynamic stability of kinematically immobile, but elastic, bodies. Let us first define kinematic immobility.

Definition 1 *An object B held in equilibrium grasp by k finger bodies is completely immobile if its configuration q_0 is isolated from the remainder of the freespace by the fingers’ c -obstacles. B is immobile to 1st order if $m_{q_0}^1 = 0$, and is immobile to 2nd order if $m_{q_0}^2 = 0$.*

Recall that a grasp which is not immobilized to 1st order may be immobilized when 2nd order effects are taken into account. The undeformed bodies are assumed to contact at a point. A contact is termed *generic* if the surfaces generated by the 2nd order approximation to the bodies' surfaces are in point contact. This requirement is almost always satisfied. Theorem 1 below relates kinematic immobility to the forces of restraint, and is a major contribution of this paper.

Theorem 1 *Let \mathcal{B} be in static equilibrium at configuration q_0 , in a generic point contact with k disjoint and stationary fingers, positioned in an essential finger arrangement. Let the finger bodies satisfy the elastic contact model (9), such that none of the fingers interpenetrates \mathcal{B} at the equilibrium. If \mathcal{B} is (kinematically) immobilized to 1st or 2nd order, the state $(q_0, 0)$ is (dynamically) locally asymptotically stable.*

Before proving the theorem we consider its physical interpretation and importance for practical applications. The theorem can be interpreted to say that if a perturbing force is applied to \mathcal{B} while \mathcal{B} is immobilized to 1st or 2nd order, then when the perturbing force is removed, \mathcal{B} is guaranteed to stabilize to its equilibrium grasp configuration with zero velocity. In particular, Mason's paradox can now be explained in terms of the temporary deformation of the decelerating finger bodies so as to generate forces opposing the motion of \mathcal{B} .

The proof of the theorem is based on the following fact. A Lagrangian mechanical system of the form

$$\frac{d}{dt} \frac{\partial}{\partial \dot{q}} K - \frac{\partial}{\partial q} K = w, \quad (8)$$

is a *damped mechanical system* when $w(t)$ is of the form $w(t) = -\nabla U(q) + f_d(q, \dot{q})$, where $U(q)$ is a potential energy function and $f_d(q, \dot{q})$ is a *dissipative vector field*. $f_d(q, \dot{q})$ is a dissipative vector field if it acts to reduce the total mechanical energy, $E = U + K$, of the system. That is, $\frac{d}{dt} E(q(t), \dot{q}(t)) < 0$ along system trajectories. Since $\dot{E} = \dot{U} + \dot{K} = \dot{U} + w \cdot \dot{q} = f_d(q, \dot{q}) \cdot \dot{q}$, $\dot{E} < 0$ whenever $f_d(q, \dot{q}) \cdot \dot{q} < 0$. We say that $f_d(q, \dot{q})$ is *negative definite at q* (with respect to \dot{q}) if $f_d(q, \dot{q}) \cdot \dot{q} \leq 0$ and $f_d(q, \dot{q}) \cdot \dot{q} = 0$ only for $\dot{q} = 0$. The stability result, attributed to Kelvin [6], is: *the local minima of U , with zero velocity, of a strictly damped mechanical system (i.e. $f_d(q, \dot{q})$ is negative definite at q) are local attractors of its flow.*

We now consider the proof for the Gesley model (the proof can be extended to any model in Section 3.2). When \mathcal{B} is contacted by k finger bodies satisfy the Gesley model, its corresponding Lagrangian dynamics are of the form (8), where $w = \sum_{i=1}^k w_i$, where

$$w_i = \begin{cases} -o_i(\eta_i \nabla o_i + \xi_i D X_{r_i}^T \dot{X}_{r_i} + \xi_i D X_{s_i}^T \dot{X}_{s_i}) & o_i > 0 \\ 0 & o_i = 0, \end{cases} \quad (9)$$

\mathcal{B} is consequently subjected to a potential energy $U(q) = \sum_{i=1}^k \frac{1}{2} \eta_i o_i^2(q)$. It is also subjected to a dissipative vector-field of the form $f_d(q, \dot{q}) = -\sum_{i=1}^k \xi_i o_i (D X_{r_i}^T \dot{X}_{r_i}(q, \dot{q}) + D X_{s_i}^T \dot{X}_{s_i}(q, \dot{q}))$.

Proof of Theorem 1: The potential energy of \mathcal{B} is $U(q) = \sum_{i=1}^k \frac{1}{2} \eta_i o_i^2(q)$. $U(q_0) = 0$, since $o_i(q_0) = 0$ for $i = 1, \dots, k$. Let $q(t)$ be a smooth c-space path such that $q(0) = q_0$. By definition, 1st order immobility implies that $\frac{d}{dt} \Big|_{t=0} d_i(q(t)) < 0$ for some $1 \leq i \leq k$. Similarly, 2nd order immobility implies that either $\frac{d}{dt} \Big|_{t=0} d_i(q(t)) < 0$ for some $1 \leq i \leq k$, or $\frac{d}{dt} \Big|_{t=0} d_j(q(t)) = 0$ for $j = 1, \dots, k$ and then $\frac{d^2}{dt^2} \Big|_{t=0} d_i(q(t)) < 0$ for some $1 \leq i \leq k$. In either case at least one d_i becomes negative after $t = 0$, which implies that at least one o_i becomes positive after $t = 0$. Thus $U(q(t))$ is locally increasing along any path $q(t)$, and q_0 is consequently a strict local minimum of U . This establishes the first requirement of the stability theorem.

Next we check if $f_d(q, \dot{q})$ is negative definite. By the chain rule, $\frac{d}{dt} X_{r_i}(q(t)) = [D X_{r_i}(q)] \dot{q}$ and $\frac{d}{dt} X_{s_i}(q(t)) = [D X_{s_i}(q)] \dot{q}$. Hence,

$$\begin{aligned} f_d(q, \dot{q}) \cdot \dot{q} &= -\sum_{i=1}^k \xi_i o_i (\dot{X}_{r_i}^T D X_{r_i} \dot{q} + \dot{X}_{s_i}^T D X_{s_i} \dot{q}) \\ &= -\sum_{i=1}^k \xi_i o_i (\|\dot{X}_{r_i}\|^2 + \|\dot{X}_{s_i}\|^2). \end{aligned} \quad (10)$$

Since $o_i > 0$ for at least one i , f_d is dissipative except when $\dot{X}_{r_i} = \dot{X}_{s_i} = 0$. Since it is possible for \dot{X}_{r_i} and \dot{X}_{s_i} to be zero for nonzero \dot{q} , it follows that f_d is only *negative semi-definite*, since $f_d(q, \dot{q}) \cdot \dot{q}$ might vanish for non-zero \dot{q} . However, it can be shown [11] that $f_d(q, \dot{q}) \cdot \dot{q}$ can vanish for non-zero \dot{q} only at isolated points of time. A simple extension of Kelvin's stability result reveals that $(q_0, 0)$ is locally asymptotically stable in such situations as well.

5 Simulations

Consider a planar object which is "grasped" by two disc-like fingers (Fig. 7). The 1st order mobility of this grasp is $m_{q_0}^1 = 2$. However, because of the concavity at the contact points, the object is immobilized to 2nd order. Thus, 2nd order effects play an important role in this example. The object's center of mass is located at its geometric center of symmetry, where the object frame is also located. Further, we assume the Gesley-like elastic deformation model and the generalized damping model of Section 3.3. That is, we implement the dynamics of Eq.s (8) and (9). Other elastic deformation models lead to analogous results. The dynamic constants are: $m = 0.5$, $I_{\theta, \theta} = 0.05$ (rotational inertia), $\eta = 2000$, $\xi = 800$. Fig. 8 shows the time histories of the x , y , and θ coordinates of the object frame for a situation in which the object is perturbed by 0.1 units in the y direction, and then released at $t = 0$. As seen in the simulations, the object does indeed converge back to the equilibrium state at $(x, y, \theta) = (0, 0, 0)$.

6 Summary and Applications

We have shown [12] that curvature effects can act to lower the mobility of a grasped object (as predicted

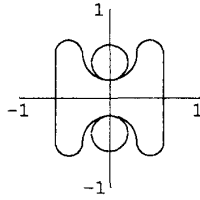


Figure 7. Two fingered planar grasp which is 2^{nd} order immobile, but has 1^{st} mobility of 2.

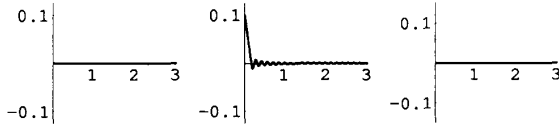


Figure 8. x , y , and θ (in radians) coordinates versus time (in seconds).

by 1^{st} order theories). Hence, 2^{nd} order effects can be used for the purposes of immobilization. However, we showed (via Mason's paradox) that rigid body models are not adequate to explain the origin of contact forces in systems that are immobilized by 2^{nd} order effects. Consequently, we introduced a useful class of lumped parameter c-space elastic deformation models which explain how the contact forces are generated by small deformation of the contacting bodies. According to Theorem 1, 1^{st} and 2^{nd} order kinematic immobility guarantees asymptotic stability of the "grasped" object with respect to small perturbations of its position and velocity. This result provides physical justification for applications of our 2^{nd} order mobility theory. Below are some obvious applications of this work which have motivated our investigation.

WorkHolding: In [12] we considered the use of 2^{nd} order effects to prove new lower bounds on the number of frictionless fingers necessary to immobilize an object. In this paper we justified these results from a dynamic perspective. These results have obvious uses for *fixture planning*. Our 2^{nd} order mobility results suggest that many objects can be immobilized with fewer numbers of fixtures than previously thought possible.

Differentiating Between Equilibrium Grasps: The 2^{nd} order mobility index can differentiate between alternate grasps that are equivalent to 1^{st} order. A careful grasp planner should choose the most secure grasps, i.e. those with the lowest 2^{nd} order mobility.

Quasi-Static Posture Planning: Current motion planners are not equipped to handle the problem of planning the motion of a mobile articulated robot in a stationary piecewise rigid environment. Examples are a "snake-like" robot that crawls inside a tunnel by embracing against the tunnel walls, or a "monkey-like" limbed robot that climbs a trussed structure by pushing and pulling. In these examples, one must plan the

robot's motion to satisfy high-level goals while maintaining *quasi-static stability*. We are primarily concerned with planning the "hand-hold" states (analogous to the hand-holds used by rock climbers between dynamically moving states) where the grasped object, or the robot mechanism in the dual case, is at a static equilibrium. We term this problem the *quasi-static posture planning* problem. Our analysis is useful for these problems because we may map the mechanism-environment pair to a dual fingers-object pair. A cautious locomotion planner will always look for equilibrium postures that minimize the mechanism's mobility.

Acknowledgments: This work was supported by Office of Naval Research Young Investigator Award N00014-92-J-1920. The authors would also like to thank Prof. Matt Mason for calling our attention to the ellipse paradox.

References

- [1] H. Hertz (1882). On the contact of elastic solids. In *Miscellaneous Papers by H. Hertz*. Macmillan, London, 1896.
- [2] B. R. Donald and D. K. Pai. On the motion of compliantly-connected rigid bodies in contact, part ii: A system for analyzing designs for assembly. In *Proc. IEEE Int. Conf. on Robotics and Automation*, pages 1756-1762, Cincinnati, OH, May 1990.
- [3] A. Gesley. From cad/cam to simulation: Automatic model generation for mechanical devices. In P. Fishwick and R. Modjeski, editors, *Knowledge-Based Simulation: Methods and Applications*. Springer-Verlag, 1989.
- [4] J. Halling. *Principals of Tribology*. Macmillan, London, 1975.
- [5] H. Hanafusa and H. Asada. Stable prehension by a robot hand with elastic fingers. In *Proc. 7th Int. Symp. Industrial Robots*, pages 384-389, 1977.
- [6] D. E. Koditschek. The Application of Total Energy as a Lyapunov Function for Mechanical Control Systems. In J. Marsden, Krishnaprasad, and J. Simo, editors, *Control Theory and Multibody Systems*, volume 97, pages 131-158. AMS Series in Contemporary Mathematics, 1989.
- [7] M. Mason. personal communication, May 1993.
- [8] D. J. Montana. The kinematics of contact with compliance. In *Proc. IEEE Int. Conf. on Robotics and Automation*, pages 770-774, 1988.
- [9] D. J. Montana. Contact stability for two-fingered grasps. *IEEE Transactions on Robotics and Automation*, 8(4):421-230, 1992.
- [10] V. T. Rajan, R. Burridge, and J. T. Schwartz. Dynamics of rigid body in frictional contact with rigid walls. In *Proc. IEEE Int. Conf. on Robotics and Automation*, pages 671-677, Raleigh, North Carolina, April 1987.
- [11] E. Rimon and J. W. Burdick. Curvature effects of bodies in contact: Their impact on mobility and their forces of restraint. Tech report, ME Department, California Institute of Technology, Sept 1993.
- [12] E. Rimon and J. W. Burdick. Mobility of bodies in contact—i: A new 2^{nd} order mobility index for multiple-finger grasps. In *Proc. IEEE Int. Conf. on Robotics and Automation*, San Diego, CA, May 1994.